Isoelastic Cable for Tension Band Fixation of Transverse Olecranon Fractures: A Biomechanical Study[1]

Fixation of olecranon (elbow) fractures is currently performed using two k-wires in addition to a stainless steel wire in a loop or figure-of-eight configuration. The SuperCable has been proposed for use in the fixation of these types of fractures as an alternative to stainless steel wire, which may cause irritation of the soft tissues surrounding the elbow.

A series of tests was performed using two k-wires with stainless wire (Figure 1a,b) or the SuperCable (Figure 1c,d) in a loop or figure-of-eight configuration for fixation of this type of fracture in cadaveric bones.

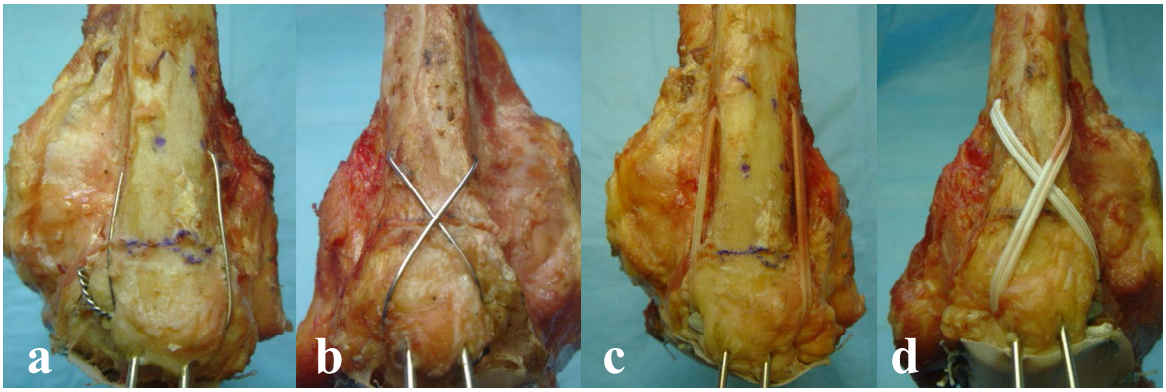

Figure 1

Cyclic loading as would be experienced during daily living was applied to each of the cadaveric elbow specimens, and the resulting motion at the fracture was measured for both the SuperCable and stainless wire constructs. Four loading cycles were performed, and the displacement at the fracture was measured under load at the end of each of the four cycles:

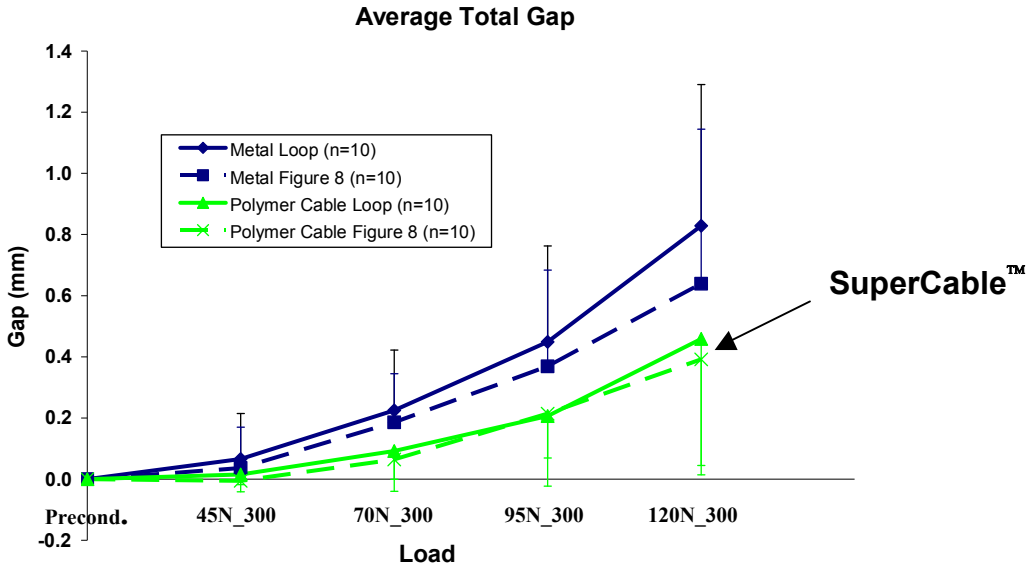

Figure 2 Average displacements (gap) of the SuperCable constructs were less than those of the stainless wire

As shown in Figure 2, the average displacement of the fracture when using a SuperCable in a loop or figure-of-eight configuration was less than the average displacement of the fracture when a stainless steel wire was used in either a loop or figure-of-eight configuration.

This study demonstrates that the SuperCable should be considered as an alternative to a stainless wire for fixation of transverse olecranon fractures and may provide better biomechanical performance than a stainless wire for tension band fixation.

The study includes a case report in which the SuperCable was used clinically for fixation of an olecranon fracture. The case involved a 73 year old female who suffered an elbow fracture following a ground level fall (Figure 3). The fracture was stabilized using a SuperCable in a figure-of-eight configuration (Figure 4a). Post-operative radiographs show reduction of the fracture and demonstrate the transparency of the cable on radiographic imaging (Figure 4b). At six-months follow-up the patient was pain free and had recovered functional use of her arm.

Figure 3 Pre-operative radiograph showing displaced olecranon fracture

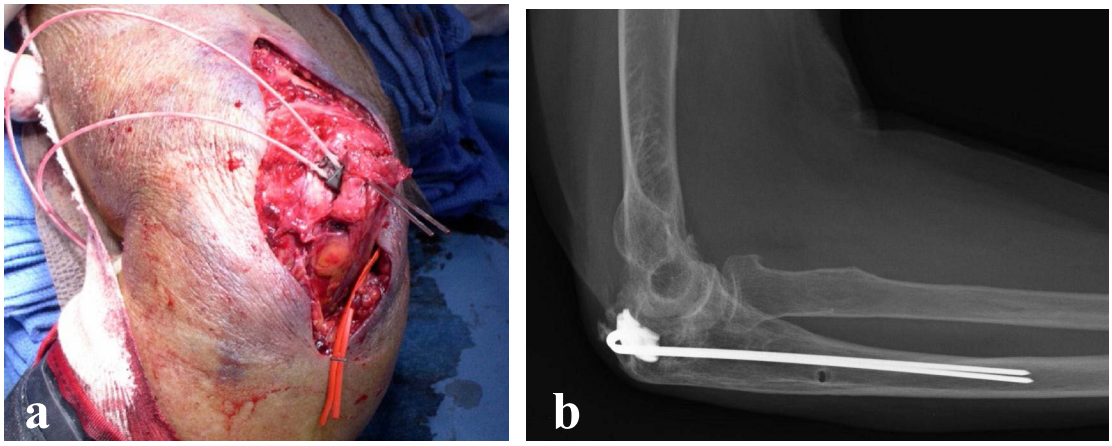

Figure 4 a) Intra-operative use of SuperCable for fixation of an olecranon fracture
b) Post-operative radiograph showing reduction of the fracture

1. Riansuwan, K., et al., *Isoelastic Cable for Tension Band Fixation of Transverse Olecranon Fractures: a Biomechanical Study, White Paper*

WHITE PAPER

Isoelastic Cable for Tension Band Fixation of Transverse Olecranon Fractures: a Biomechanical Study

Kongkhet Riansuwan MD[1, 2], Joy C Vroemen[1], Halil Bekler MD[1], Jason McKean MD[1], Valerie M. Wolfe MD[1], Thomas Gardner MCE[1], Melvin P Rosenwasser MD[1]

[1] Trauma Training Center and Center for Orthopaedic Research
Department of Orthopaedic Surgery, Columbia University Medical Center
New York, NY

[2] Department of Orthopaedic Surgery
Faculty of Medicine Siriraj Hospital, Mahidol University
Bangkok, Thailand

Abstract:

This biomechanical study was conducted to compare the stability of tension band fixation of transverse olecranon fractures with isoelastic polymer cable to the stability of tension band fixation with stainless steel wire. Ten matched pairs of fresh-frozen cadaveric elbows without radiographic abnormality were selected for the study. A transverse fracture model was simulated in each specimen with an osteotomy at the middle part the greater sigmoid notch of the olecranon. One elbow of each pair was randomized for tension band fixation with figure of eight cerclage while the other was fixed with circular loop cerclage. Two materials, stainless steel wire and isoelastic polymer (polyethylene-nylon composite) cable, were used to sequentially create the cerclage constructs in each elbow pair, with the order of material type randomized. The stability of each construct was tested with a series of cyclic loads to the ulna. A preconditioning period of 100 cycles at 45 N was followed by a series of 300 cycles of cyclic loadings at 45 N, 70 N, 95 N and 120 N. The loads were applied to the dorsal cortex of the ulna to create a bending moment at the fracture site. Dynamic and static fracture gapping, as well as articular step-off were recorded and compared between the different configurations and materials. No difference in static gap was found between the metal figure-of-eight, cable figure-of-eight, and cable loop constructs ($p>0.05$). The metal loop was found to have significantly greater gapping ($p=0.0013$) than the other 3 constructs. There were no differences in mean dynamic gap ($p=0.0670$), peak dynamic gap ($p=0.3379$) and articular step-off ($p=0.1501$) among the four constructs. This study demonstrated that the biomechanical performance of tension band fixation in a cadaveric olecranon fracture model using a polymer cable in either figure-of-eight or loop construct is similar to that of the stainless steel wire figure-of-eight construct and should be considered as an option to the traditional stainless steel wire. The material properties of the polymer cable fixation may lessen the known clinical complications of wire fixation while providing equivalent stability under physiologic loads and permitting early rehabilitation.

Keywords:

olecranon fracture, tension band fixation, isoelastic cable, biomechanics, elbow

WHITE PAPER

Brief Title:

Isoelastic Polymer Cable Fixation of Olecranon Fractures

INTRODUCTION

Olecranon fractures are one of the most common fractures of the upper extremity.[1] The goals of treatment in such fractures are to anatomically reduce the fracture, stabilize and promote healing, maintain function of the elbow, and prevent complications.[2] Operative treatment by open reduction and internal fixation is often necessary to achieve these goals. Tension band wiring is one of the most common methods of internal fixation utilized in simple transverse olecranon fractures.[3] The traditional approach has been to combine a stainless steel wire with two Kirschner wires (K-wires) to create the tension band construct.[4]

The tension band construct may be made in various ways including K-wires placed intramedullary in the ulna or exiting the anterior cortex distal to the coronoid. Mullett et al. studied the biomechanics and clinical outcomes of both techniques.[5] It appeared that K-wires exiting through the anterior cortex technique resulted in greater pull-out strength and fewer complications requiring K-wire removal than the intramedullary technique. However, the senior investigator in our study prefers to use intramedullary K-wire fixation because of the potential clinical risks of neurovascular injury and limitation of elbow motion by anterior blocking from the protruding K-wire tip.

Despite generally good results with stainless steel wire tension band constructs, adverse events associated with the stainless steel wire such as poor conformation, wire breakage, kinking, and skin irritation with the wire knot have been reported in the literature[6-8]. These complications may cause patient pain and can often lead to secondary procedures for implant removal. Different materials have been investigated in attempts to eliminate these problems.[9] However, no other material has been shown to possess mechanical properties superior to those of stainless steel wire.[10]

Iso-elastic cable is a new kind of polymer cable made from ultra-high molecular weight polyethylene (UHMWP) strands braided over a nylon core. This cable is more elastic, pliable, conformable, and has a higher fatigue strength than that of metal wire or braided metal cable.[11] Braided polyethylene cable, without a nylon core, has been tested against stainless steel in animal biomechanical studies and has demonstrated comparable mechanical properties without suffering wear-related breakage.[12] Additionally, polyethylene cable, also without a nylon core, has been used for spinal cerclage [13]. This study will investigate the efficacy of an iso-elastic polymer (polyethylene-nylon composite) cable in our construct of tension band wiring for fixation of transverse olecranon fractures in a cadaveric human model.

MATERIALS AND METHODS

A series of pilot studies were conducted using 6 unpaired fresh frozen human elbows and 4 paired fresh frozen human elbows, for a total of 14 pilot elbows, to establish the proper fixation techniques, loading profiles and method of gap fixation that resulted in repeatability.

Following the pilot studies, ten matched pairs of fresh frozen human elbows without radiographic abnormality were selected for data collection. These included 7 male and 3 female arms with an average age of 56.7 (range 52 to 79). Each elbow was wrapped with saline-soaked towels and kept at -20^{o} C, and the freeze/thaw cycle was controlled prior to dissection and testing. After thawing at room temperature, each specimen was transected at the level of the mid-arm and forearm. All soft tissues were removed except for the triceps mechanism, joint capsule, and medial and lateral collateral ligaments. Each specimen was positioned within a 1-1/2" diameter x 3" length threaded steel pipe. To prevent rotation of the specimen, the distal humerus was fixed to the pipe using a machine screw. The bone was then secured within the pipe by filling the pipe with expansion cement (Rockite, Hartline Products Co., INC. Cleveland, Ohio).

Fracture Model

A transverse fracture model of the olecranon was simulated as described by Molloy.[14] An osteotomy was performed at the center of the olecranon process. The osteotomy was initially carried out from dorsal cortex down to the subchondral bone using an oscillating saw (Arthrex AR-8250 with a 0.5 mm-thick saw blade) and then completed with a sharp osteotome to create a fracture model through the articular cartilage. For each matched pair of elbows (right and left from a single cadaver), one elbow was randomized for fixation with a tension band construct (modified AO technique) with figure-of-eight cerclage (Figure 1) while the other side was fixed with circular loop cerclage (Figure 2). Two test materials were used: 18-gage 316Lstainless steel monofilament surgical wire (Zimmer, Warsaw, IN) and double strands of 1.5 mm iso-elastic polymer cable (SuperCable, Kinamed, Inc., Camarillo, CA). Two-block randomization was used to assign one of the two materials to each cadaver, and figure-of-eight versus loop configuration was kept on the same side (right versus left) in each block.

For modified AO figure-of-eight tension band fixation, the fracture was reduced and two parallel K-wires (0.0787"; 2.0 mm, Zimmer, Warsaw, IN) were used to maintain the fracture. Both K-wires were passed from the tip of the olecranon to purchase the anterior cortex of the proximal ulna around the base of the coronoid process under C-arm guidance. The distance between the K-wires was 1 cm, and the K-wire length beyond the fracture site was approximately 2 times the distance from the olecranon tip to the fracture site.[15]

For the stainless steel wire cerclage, a bicortical anchor hole was created by a 3.5 mm drill bit at the posterior cortex of the proximal ulna. This was done at the same distance distal to the osteotomy site that the osteotomy was from the olecranon tip. One end of the stainless steel wire was then passed through the hole; another end was passed around the K-wires and under the triceps tendon in loop or figure-of-eight as appropriate. The wire was tightened and twisted by using the one knot technique. The twisting force was controlled at 50 ounce-inches by using a torque-limiting screw driver with a custom tip (model UTICA TS-100, Cooper Power Tools, Hicksville, OH). For the iso-elastic cable cerclage, pilot testing showed a tendency of the cable to cut through the bone when the bi-cortical anchor hole was located approximately the same distance from the fracture site as the fracture was from the tip of the olecranon. To prevent this from occurring in the test samples, the 3.5 mm bicortical anchor hole was placed approximately twice the distance along the posterior cortex of the ulna distal to the fracture site that the fracture site was from the tip of the olecranon using a 3.5 mm drill bit. Two strands of the cable were passed through the hole, across the fracture site and under the triceps to create either a circular loop or a figure-of-eight cerclage as appropriate. The cables were tightened with a tensioning device to 530 N and secured with a locking clasp. Fracture reduction was assessed using pre-loading and post-loading fluoroscopic imaging of posterior/anterior and lateral elbow images.

FIGURE 1

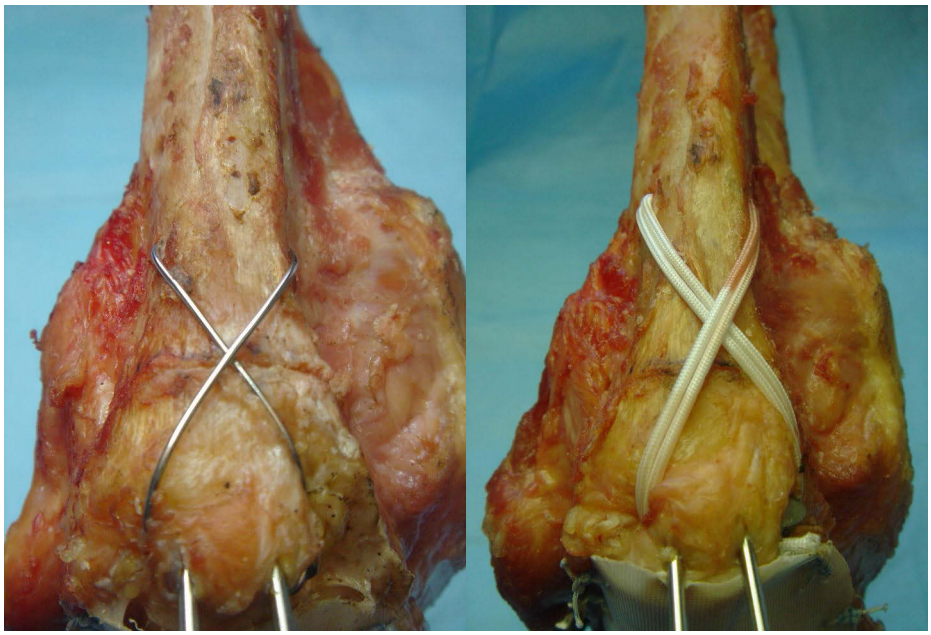

Fig. 1 Figure-of-eight cerclage fixation of an olecranon fracture model. Figure-of-eight created with 18-gage 316Lstainless steel monofilament surgical wire (left); the same figure created with double strands of 1.5 mm iso-elastic polymer (polyethylene-nylon composite) cable (right).

FIGURE 2

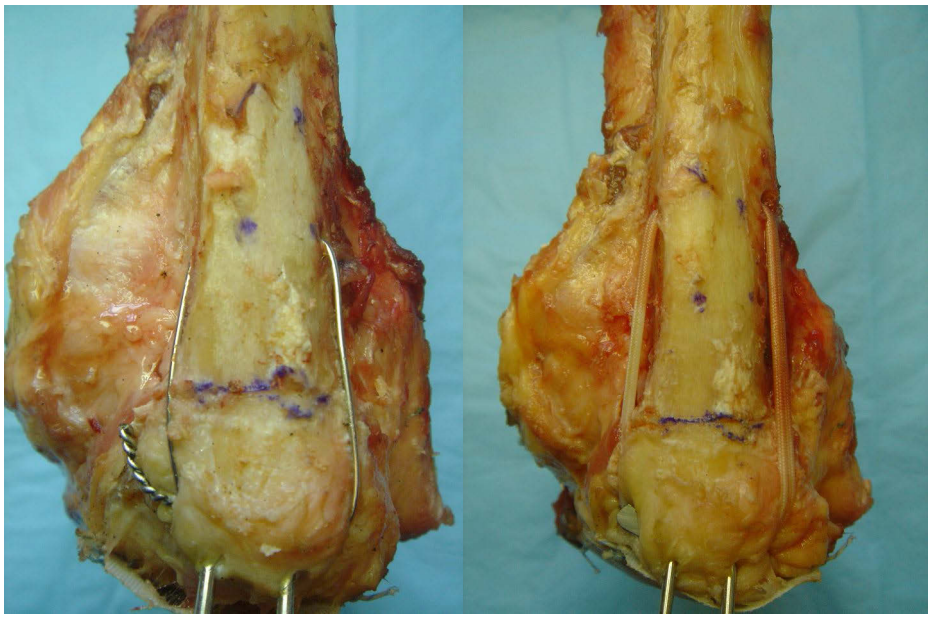

Fig. 2 Circular loop cerclage fixation of an olecranon fracture model. Figure-of-eight created with 18-gage 316Lstainless steel monofilament surgical wire (left); the same figure created with double strands of 1.5 mm iso-elastic polymer cable (right).

Mechanical Testing

Each prepared specimen was mounted to a testing apparatus as previously described by Prayson et al.[16] A microminature differential variable reluctance transducer (DVRT) with a 9 mm linear displacement response (MicroStrain, Inc., Williston, VT) was placed across the repaired simulated fracture to monitor the amount of fracture gap that occurred during loading. The body and core of the DVRT were secured to the dorsal ulnar cortex by custom-made holders and 0.9 mm K-wires driven into the bone. The resolution of the DVRT was better than 1 μm, with an accuracy of approximately 2 μm. The strength of the triceps attachment was augmented by placing the triceps tendon between the folds of Dacron sailcloth which were then secured with super glue (Loctite 416 super bonder, Loctite Crop., Rocky hill, CT) and multiple sutures (# 1 Ethibond). The augmented triceps attachment was secured to the pipe with two circular steel hose clamps at the initial elbow flexion angle of 70°. A small circular metal washer of known diameter was then attached to the medial epicondyle with a screw to control for fluoroscopic magnification and to serve as a reference scale for the fluoroscopic images used to measure intraarticular step-off.

The specimen was then secured in a MTS 858 Bionix servo-hydraulic testing machine (MTS Eden, Prairie, MN) with the humerus parallel to the direction of the machine's actuator, placing the ulna approximately perpendicular to the line of action of the actuator. A 2"-diameter solid stainless steel cylinder was attached to a 1 KN load cell, and the joints positioned such that the cylinder contacted the dorsal aspect of the ulna approximately 8.0 cm distal to the simulated fracture (Figure 3). A mini C-arm image intensifier (MiniView, GE Medical Systems OCE) was positioned to provide real-time images of the elbow in the lateral view. A series of cyclic loadings were applied to each specimen after a preconditioning period of 100 cycles at 45 N. After preconditioning, the hose clamps were retightened, and then four sequences of 300 cycles were applied to the ulna at 45 N, 70 N, 95 N and then 120 N respectively in a saw-tooth waveform at a frequency of 1 Hz. Static gapping was determined by placing a 5 N load on the ulna after preconditioning and setting the DVRT measurement with this load as zero gap. After each of the subsequent cyclic loading periods the 5 N tare load was again applied and the difference in the DVRT reading from before and after the cyclic loading period was taken as the gapping that resulted from that loading cycle. Dynamic gapping was continuously measured by the DVRT throughout the loading cycles. The DVRT data were acquired by the material testing device so that these data were synchronized with the applied load. An average mean dynamic gap over the 300 cycles of loading was computed by averaging all the mean (midway between the minimum dynamic gap and the peak dynamic gap) dynamic gaps for that loading period. Similarly, an average peak dynamic gap was computed by averaging all the peak dynamic gaps over each loading period. Articular step-off was measured in millimeters from the post-test x-ray images by using the Scion image software (Scion Corp., Frederick MD), with "significant step-off" defined as step-off greater than 2mm. The specimens were kept hydrated throughout the experiment by frequent spraying with a 0.15 M NaCl solution.

FIGURE 3

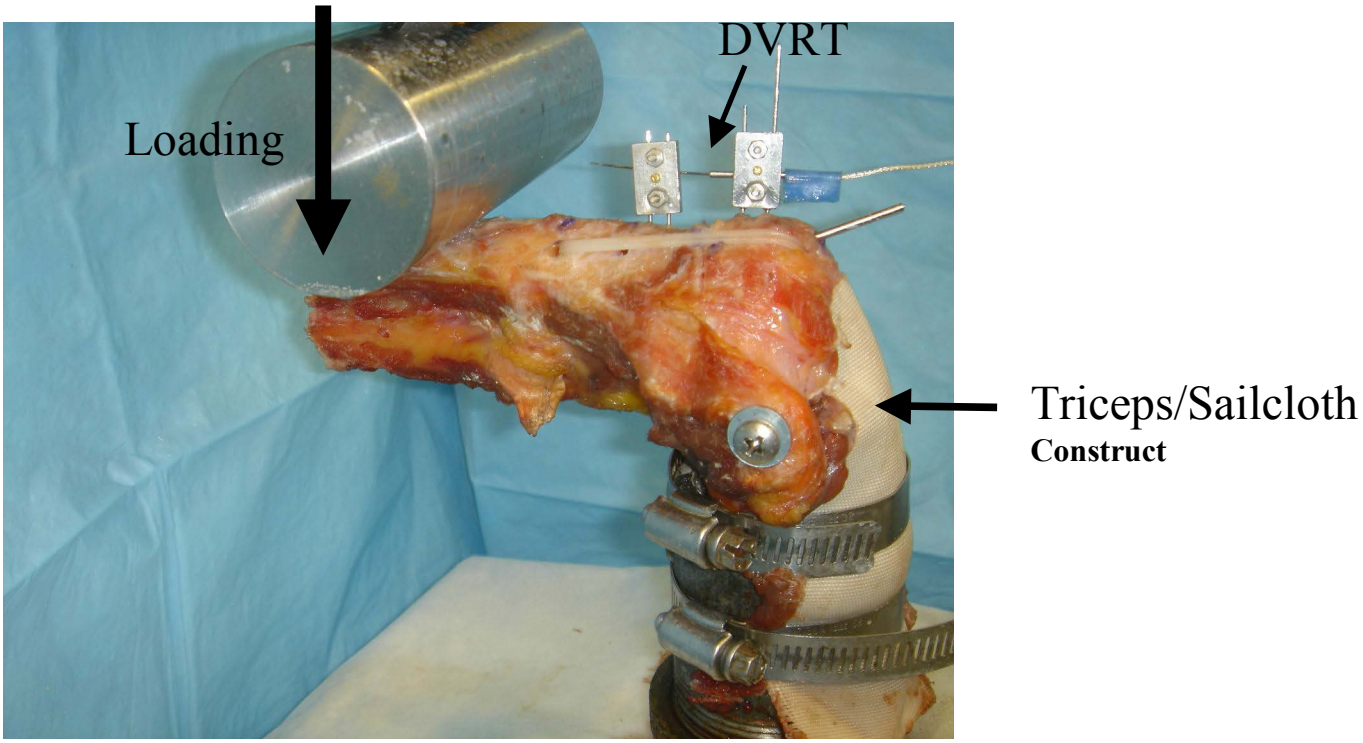

Fig. 3 A specimen is pictured as prepared for mechanical testing. A DVRT was placed across the repaired simulated fracture, and a 2"-diameter solid stainless steel cylinder attached to a 1 KN load cell was positioned so that it contacted the dorsal aspect of the ulna approximately 8.0 cm distal to the simulated fracture.

Statistical Analysis

A two-way repeated measures on both factors ANOVA was performed with material (cable, metal) as the first factor and configuration (figure-of-eight, loop) as the second factor with static gapping, mean dynamic gapping, and peak dynamic gapping as the dependent variables. The data include gapping measurements for all loading conditions (45 N, 70 N, 95 N, 120 N). A second two-way repeated measures for both factors ANOVA was performed with load (45 N, 70 N, 95 N, 120 N) as one factor and experimental construct (cable loop, cable figure-of-eight, metal loop, metal figure-of-eight) as the second factor. A Student-Newman-Keuls multiple comparisons test was used to ascertain where any statistical differences were if a statistical difference in either of the factors was found from the ANOVA. A one-way repeated measures ANOVA was performed with configuration (cable loop, cable figure-of-eight, metal loop, metal figure-of-eight) with static articular step-off as the single dependent variable. Student-Newman-Keuls multiple comparisons test was used to ascertain where any statistical differences were if a statistical difference was found from the ANOVA. Statistical significance was taken as $p<0.05$. All ANOVA were performed with the SAS® statistical software package (SAS International, Cary NC). Post-hoc power analyses were performed for the articular step-off, average mean dynamic gapping and peak dynamic gapping using the power analysis software PASS (NCSS, Kaysville Utah).

RESULTS

The average total (or cumulative) static gapping (the gap that occurs when a static 5 N load was applied to the ulnar 8 cm distal to the fracture) is shown in Figure 4. The gap is seen to increase with increasing load; this also represents an increased number of loading cycles. Both metal constructs, on average, have a greater gap than either cable construct. The difference in total gap between figure-of-eight and loop is not as pronounced as the differences between that of metal and polymer cable.

FIGURE 4

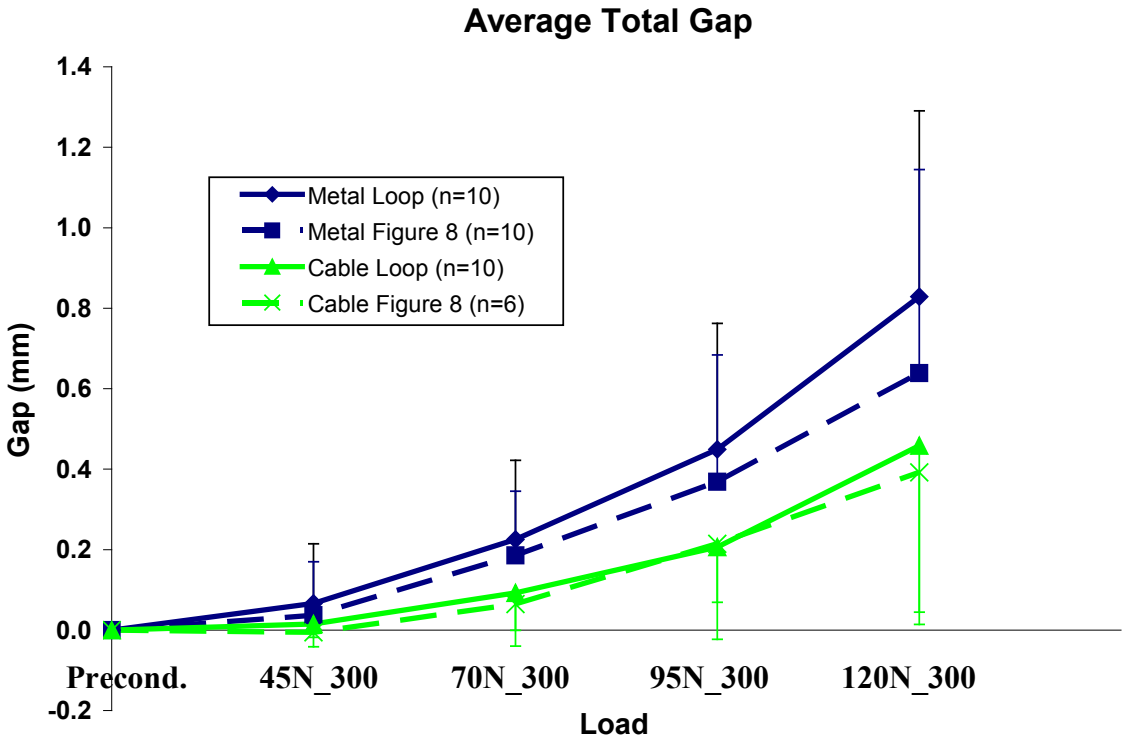

Fig. 4 The average total static gap is depicted as a function of increasing load by construct. Solid lines represent the loop configuration and dashed lines represent the figure-of-eight configuration.

When comparing the overall effect of material type on the amount of static gap formation per 300 cycle loading period (Figure 5), polymer cable (0.097 ± 0.148 mm) was found to result in a significantly ($p=0.0194$) smaller gap than the stainless steel (0.180 ± 0.223 mm). A similar, but not statistically significant effect, was found for both the average mean dynamic gap (Figure 6) and the average peak dynamic gap (Figure 7). The average mean dynamic gap formation per 300 cycles for the polymer cable (0.571 ± 0.525 mm) was less ($p=0.0727$) than that of the metal (0.808 ± 0.830 mm). Likewise, the average peak dynamic gapping per 300 cycles for the polymer cable (0.616 ± 0.610 mm) was less ($p=0.1445$) than that of the metal (0.833 ± 0.877 mm). When looking at the overall effect of the configuration of the repair, the figure-of-eight configuration resulted in significantly less ($p=0.0095$) gapping per 300 cycle loading period (0.121 ± 0.163 mm) than the loop construct (0.157 ± 0.219 mm).

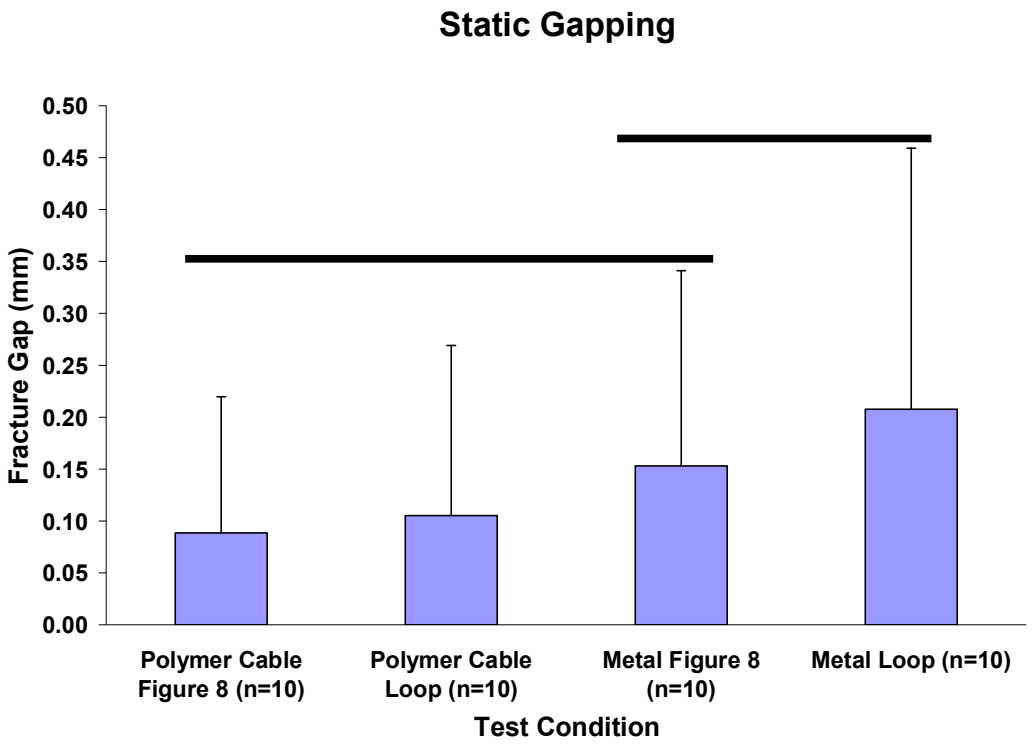

Fig. 5 The static gapping is depicted per 300 cycles of loading. Different solid bars denote statistically different groups ($p<0.05$).

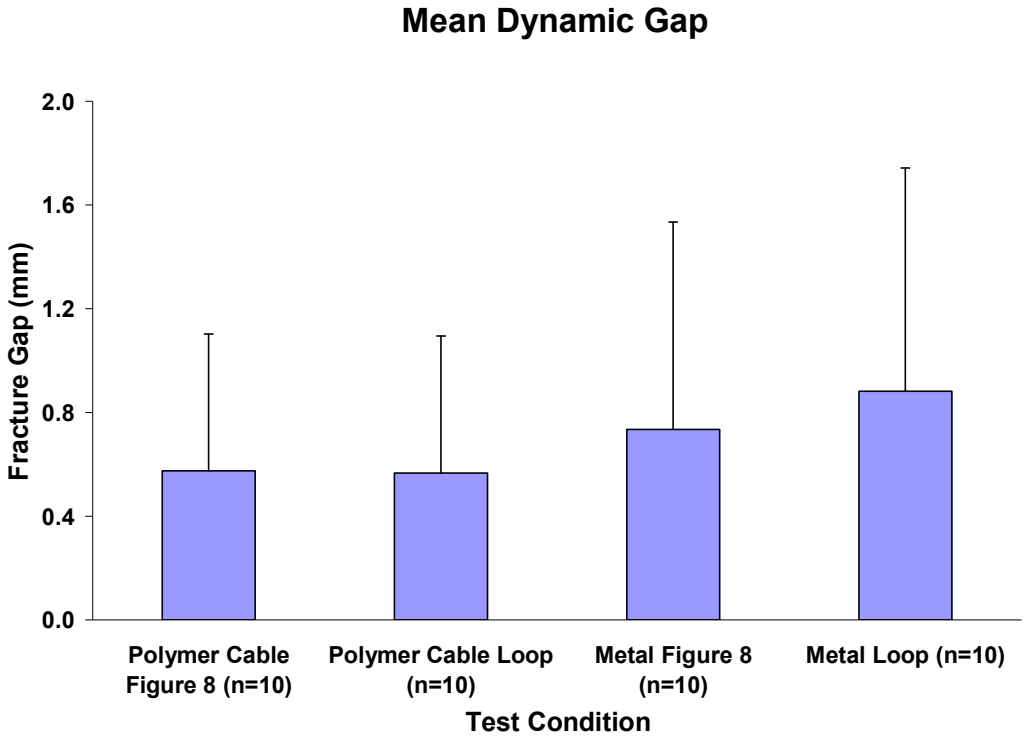

Fig. 6 The average mean dynamic gap is depicted per 300 cycles of loading. No statistical difference was demonstrated between any groups.

When looking at the overall effect of construct (cable loop, cable figure-of-eight, metal loop, metal figure-of-eight) no difference ($p>0.05$) in static gap formation per 300 cycle loading period was found between the metal figure-of-eight (0.153 ± 0.188 mm), cable figure-of-eight (0.089 ± 0.131 mm) and cable loop constructs (0.105 ± 0.164 mm). The metal loop gap (0.208 ± 0.251 mm) was found to be significantly greater ($p=0.0013$) than the gap for the other 3 constructs (Figure 5). There were no differences in mean dynamic gap ($p=0.0670$) between constructs (Figure 6). There were also no differences found between construct for the average peak dynamic gapping ($p=0.3379$; Figure 7). Not surprisingly, gapping increased with increasing load. Mean dynamic gap per 300 cycles for a 45 N load (0.347 ± 0.266 mm) was less than for 70 N of load (0.581 ± 0.446 mm) though this result did not reach statistical significance. Static gapping for the 95 N load was statistically greater ($p<0.05$) than that at 70 N, and gapping at 120 N of load (1.308 ± 1.010 mm) was statistically greater ($p<0.05$) than that at 95 N (Figure 8).

FIGURE 7

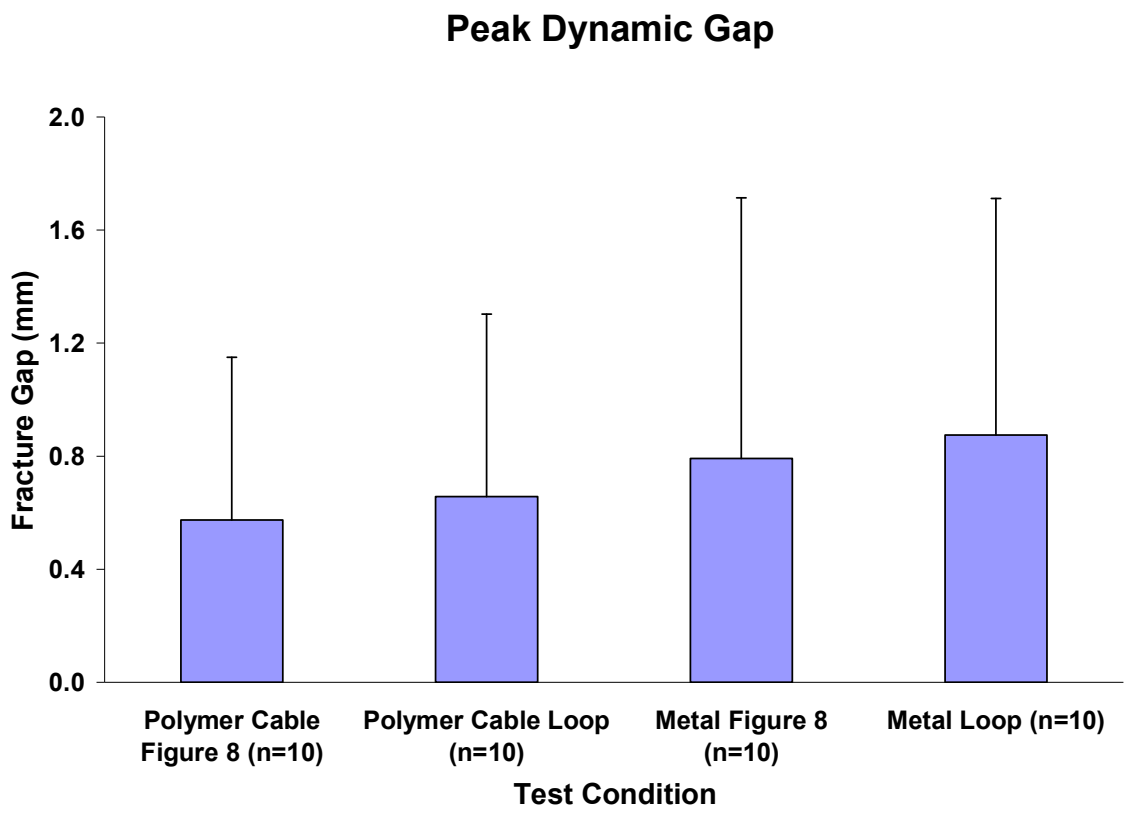

Fig. 7 The average peak dynamic gap is depicted per 300 cycles of loading. No statistical difference was demonstrated between any groups.

FIGURE 8

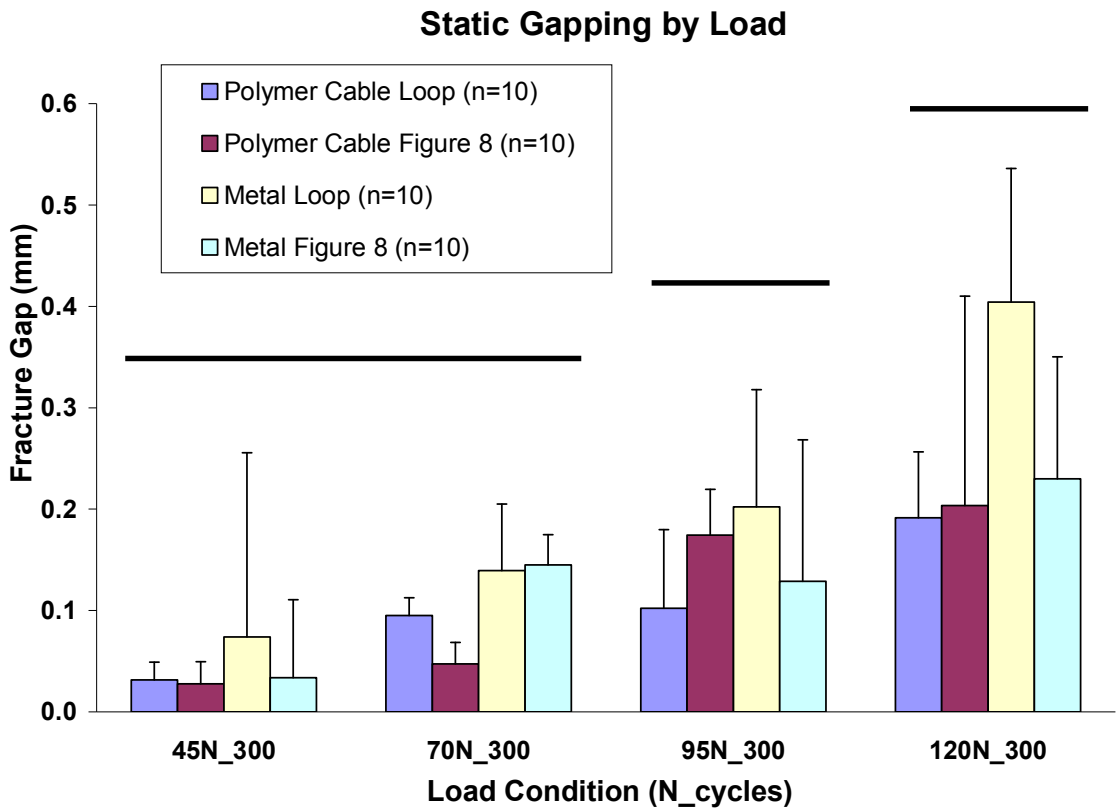

Fig. 8 Static gap is depicted by load. Different horizontal bars indicate statistically different groups, $p<0.05$.

There was also no difference in articular step-off ($p = 0.1501$) among the four constructs, though both polymer cable constructs had less step-off than for either metal construct (Figure 9).

FIGURE 9

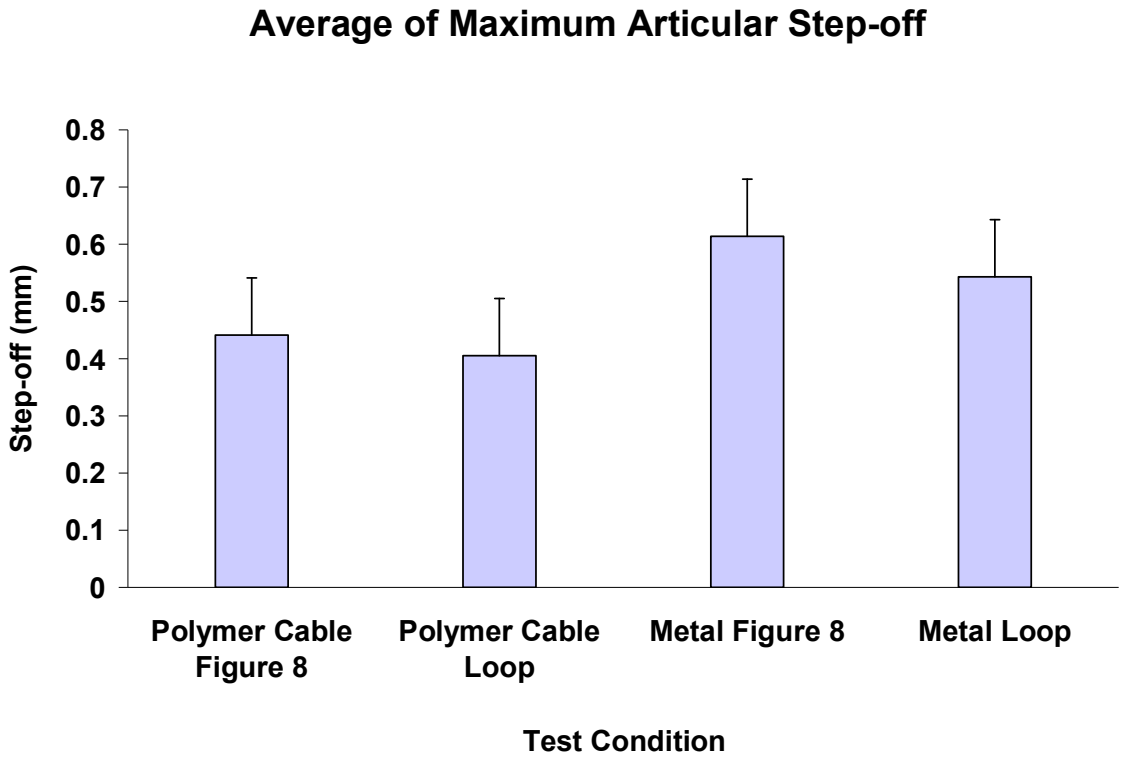

Fig. 9 Articular step-off is depicted by construct. The values represent the maximum step-off observed from radiographs taken after completion of the loading protocol.

DISCUSSION

This study demonstrated that the biomechanical performance of tension band fixation in a cadaveric olecranon fracture model using a polymer (polyethylene-nylon composite) cable in either figure-of-eight or loop construct is similar to that of the stainless steel wire figure-of-eight construct. Stainless steel tension cabling has been proven biomechanically and clinically to be a safe and effective repair construct for olecranon fractures. Biomechanically, when the constructs were grouped by material, the ioelastic polymer cable exhibited statistically ($p=0.0194$) smaller static gapping than that of the metal constructs. However, when individual constructs were considered, there was no difference in static or dynamic gapping between the isoelastic polymer figure-of-eight, polymer loop and stainless steel wire figure-of-eight constructs whereas the metal loop construct exhibited significantly greater ($p=0.0013$) static gapping. Isoelastic polymer cable should therefore be considered a biomechanically equivalent, effective alternative to the traditional stainless steel wire.

Clinically, the iso-elastic polymer cable offers multiple advantages over stainless steel. First, the cable is more similar to biologic tissue. While subcutaneous placement of stainless steel often results in irritation of tissues, the iso-elastic polymer cable is less irritating to the body. This could result in a decreased complication rate and decreased incidence of second surgery though this remains to be seen as the construct is used clinically. Second, the polymer cable is more pliable than metal, allowing the surgeon to create multiple loops with the cable without the risk of kinking that exists with metal. No double-loop is necessary to prevent the kinks from forming. Additionally, the ends of the polymer cable are not sharp like the ends of a stainless steel wire. This decreases the risk for needle and wire sticks for the surgeon and staff in the operating room. Third, the polymer cable does not appear on x-ray. Though this decreases the ability to evaluate consistency of the construct over time, it allows for better visualization of the bone and the fracture site post-operatively. The pliable nature of the polymer cable prevents kinks that can occur with metal wire, thereby assuring that the tension in the cable is more uniformly distributed than would occur with a metal wire. Furthermore, the clasp mechanism used to secure the cable allows for readjustment of the cable tension, an option that is not available with metal wire. The clasping mechanism also negates the need for burying the knot that exists when the ends of the metal wire are twisted. Since a tension device is used to set, and if needed, reset the tension in the cable, the tension can be more easily controlled than for the wire, where no quantitative feedback is used as the metal is twisted to create tension in the wire. One disadvantage was noted with the clasp, in that it tended to migrate as the load was applied to the cable or as the cable was tightened on the elbow. A desirable modification to the clasp would be the addition of prongs or some mechanism that would allow the clasp to stay fixed. As noted in the above text, there was a potential disadvantage of the tendency of the cable to cut through the bone when the bicortical anchor hole was located the same distance from the fracture site as the fracture was from the tip of the olecranon. This was easily remedied by placement of the anchor hole at twice this distance.

The clinical advantages of iso-elastic polymer cable tension band constructs have been observed by the senior investigator in two procedures involving elbow fracture repair. One representative case involved a 73 year old female who suffered a ground-level fall that resulted in a grade I open Monteggia fracture dislocation. Pre-operative radiographs revealed marked comminution of the proximal ulna and instability with posterolateral displacement of the radiocapitellar joint (Figure 10). Intraoperatively, the fracture was stabilized using iso-elastic polymer cable in a figure-eight configuration (Figure 11). Post-operative radiographs demonstrate adequate reduction and show the complete transparency of the iso-elastic polymer cable on radiographic imaging (Figure 12). This patient went on to recover 150° of extension, 50° of flexion, 65° of supination, and 80° of pronation at six-month follow-up (Figure 13). The patient also reported ‘no pain’ at the site of the fracture. Though there was no statistical difference found in gapping between the cable loop and cable figure-of-eight constructs from the cadaveric biomechanical testing, the personal preference of the senior author is the figure-of-eight constructs. It was felt that this construct provided better stability and ease in application.

There were several limitation in this study, the primary of which is the low number of arms used. Even with ten matched pairs, the power of the study to detect a significant difference specific to each variable is not much greater than 50%. For example, the power to detect a 25% difference in the means between the four construct types (cable loop, cable figure-of-eight, metal loop, metal figure-of-eight) for the average static gap was approximately 0.21. For a 50% difference in the means of these constructs, the power was 0.7. Therefore, the risk of Type II error is not small and hence it is possible that relatively small, but not insignificant, differences may exist that were not detected.

FIGURE 10

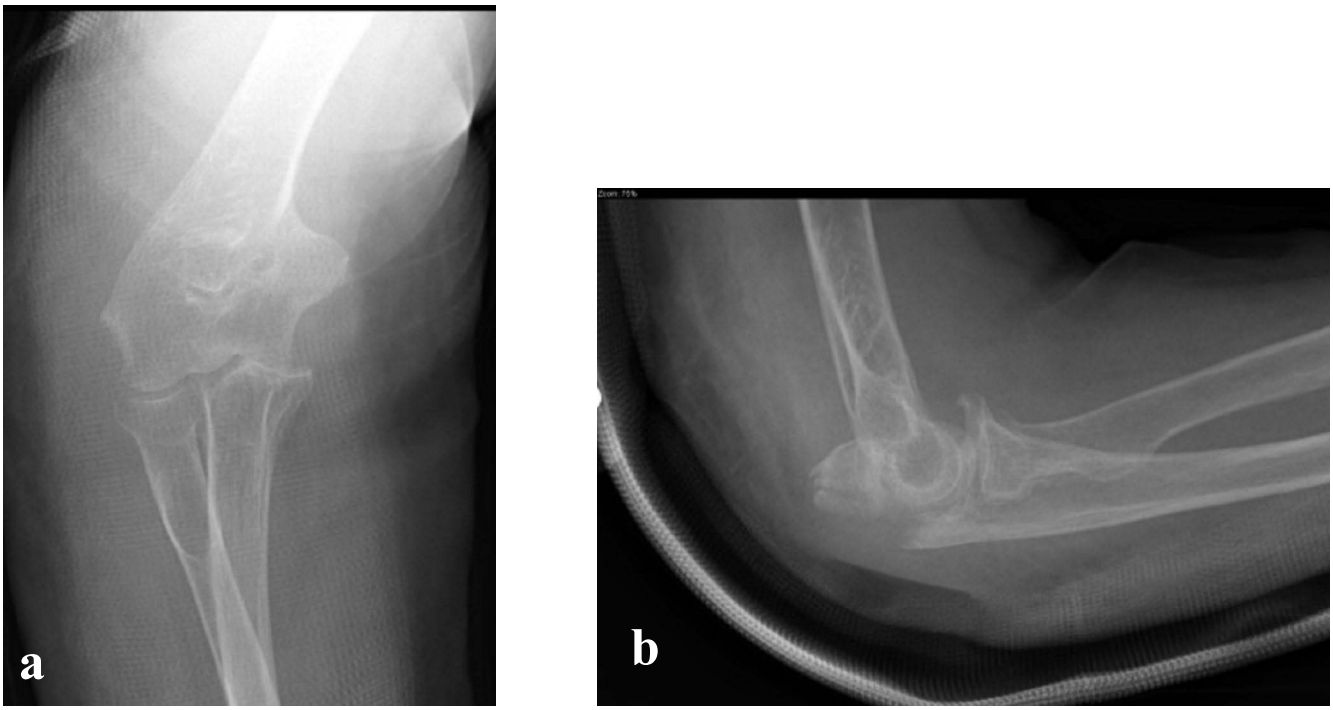

Fig. 10 Pre-operative radiographs with a) AP and b) lateral views. These demonstrate a grade I open Monteggia fracture dislocation from a ground-level fall showing marked comminution of the proximal ulna and instability with posterolateral displacement of the radiocapitellar joint.

Since the amount of elbow flexion was set by securing the augmented triceps construct, viscoelastic creep and likely microdamage to the triceps allowed the degree of flexion of the elbow to increase with increasing load and time. This changed the direction of the loading vector applied by the circular cylinder. To minimize this, the elbow was repositioned after the preconditioning period. This greatly reduced the amount of increased flexion for the reminder of the test for most specimens, but some specimens did exhibit increased flexion angles at the high loading levels.

Another limitation was the way in which the gapping was measured. The DVRT can only measure linear translation. However, the gap represents an increase in distance due effectively to a rotation. Because of this, the DVRT experiences a small amount of bending when large gaps occur. The friction is minimal with the DVRT so there is little chance that any loss of displacement occurred because of sticking. The bending of the DVRT does represent a portion of the displacement that is not properly accounted for. However, since the length of the DVRT is relatively short, and the attachment sites of the DVRT were relatively close to the edges of the gap, the amount of bending was minimized and any loss of translation, and hence gap, is felt to very small compared to the gaps that occurred at the higher loads. The amount of variation in the gapping was more pronounced for the dynamic gapping measurements than for the static measurement because of the motion of the ulna as it was cyclically loaded. Since the elbow is not a true pin joint, there was also slight motion perpendicular to the plane of loading, which introduced additional noise to the DVRT measurements. However, this motion was generally fairly small and is felt not to have any significant effect on the overall results.

Finally, it was assumed that there was no difference between the left and right arms of the paired specimens so that a repeated measures ANOVA could be performed for all four constructs. The construct type was randomized between left and right arms to minimize any impact of this assumption.

FIGURE 11

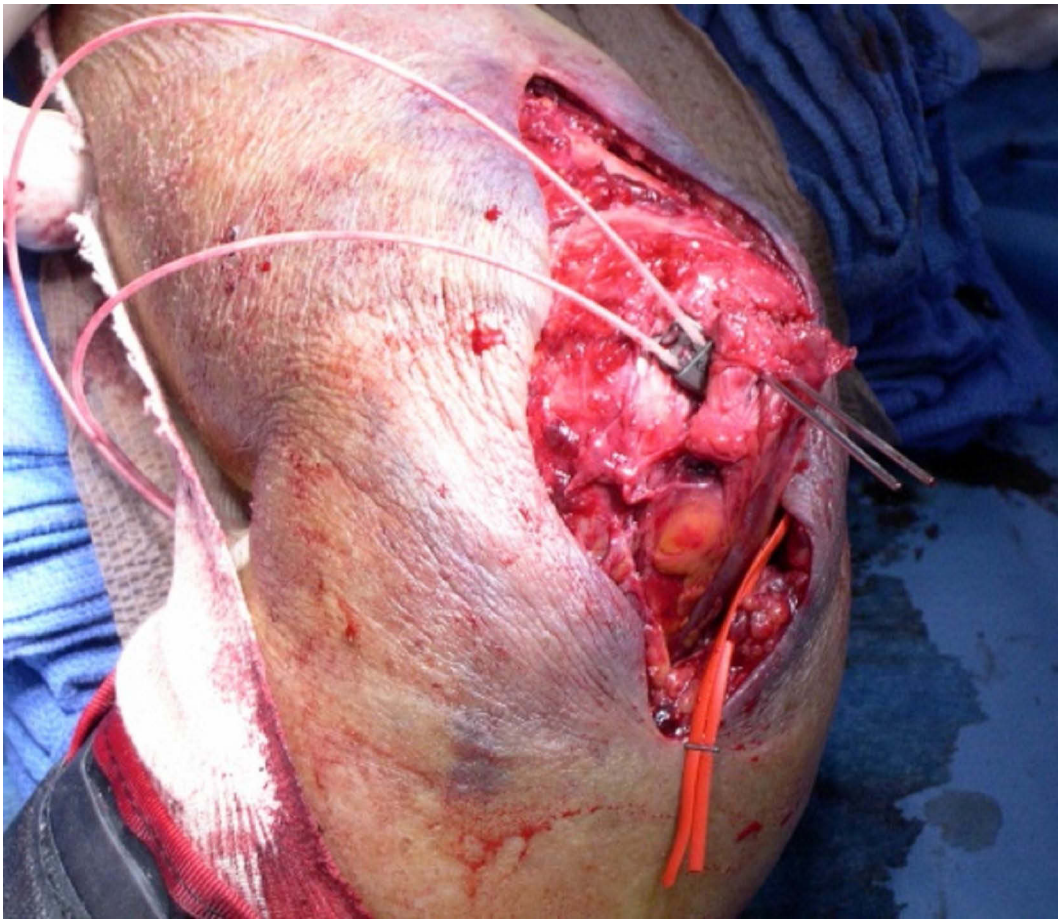

Fig. 11 Intra-operative demonstration of the use of the polymer cable.

Conclusions

This study demonstrated that the iso-elastic polymer (polyethylene-nylon composite) cable should be considered as an option to traditional stainless steel wire in tension band fixation of transverse olecranon fractures. The biomechanical performance of the polymer cable in either figure-of-eight or loop construct is better than or similar to that of the stainless steel wire figure-of-eight construct in limiting gap formation after cyclic loading in a cadaver model. The soft-tissue tolerant fixation achieved with the polymer cable may lessen the known clinical complications of wire fixation while providing equivalent stability under physiologic loads to permit early rehabilitation.

FIGURE 12

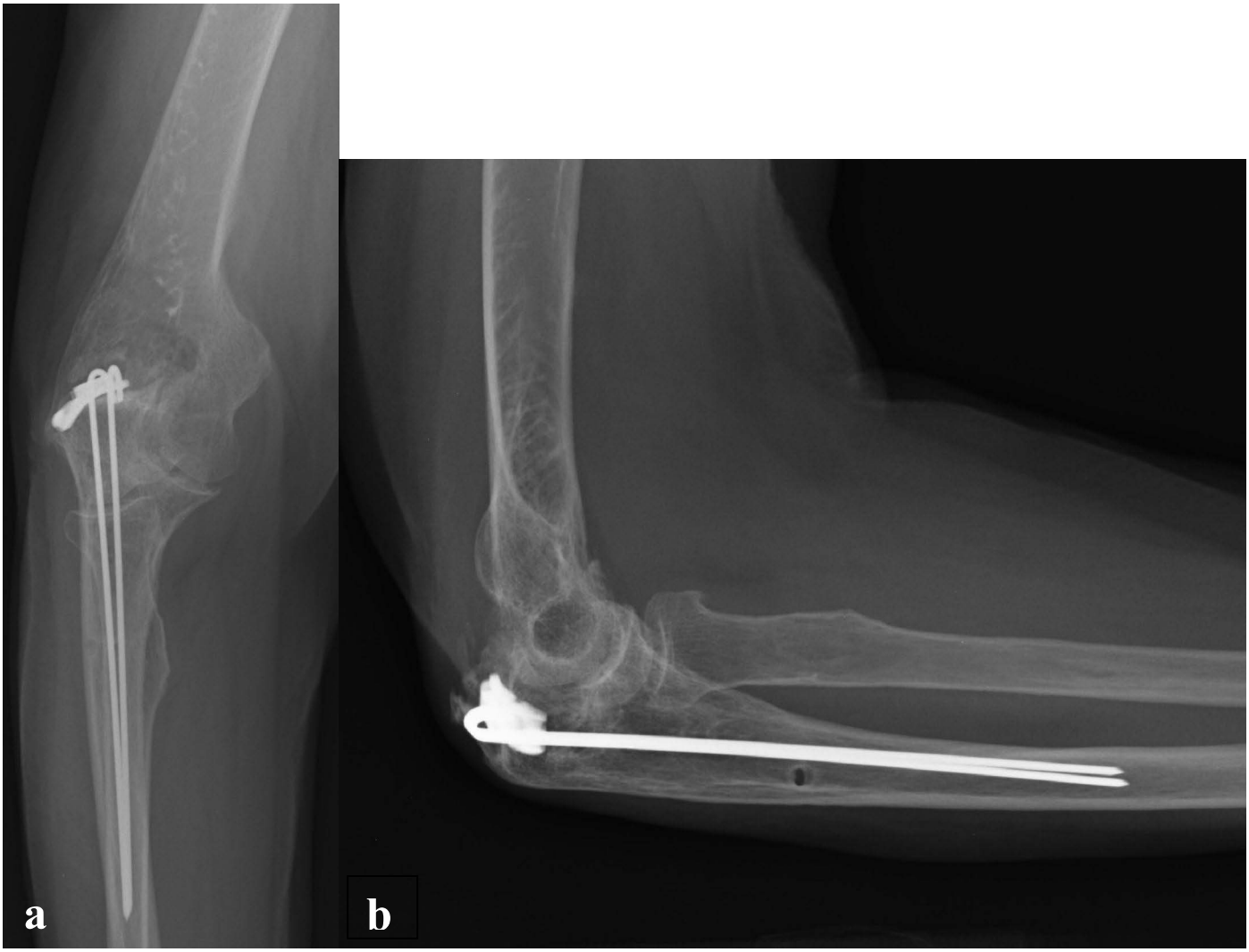

Fig. 12 Post-operative radiographs with a) AP and b) lateral views. The images demonstrate adequate reduction and show the complete transparency of the iso-elastic polymer cable.

FIGURE 13

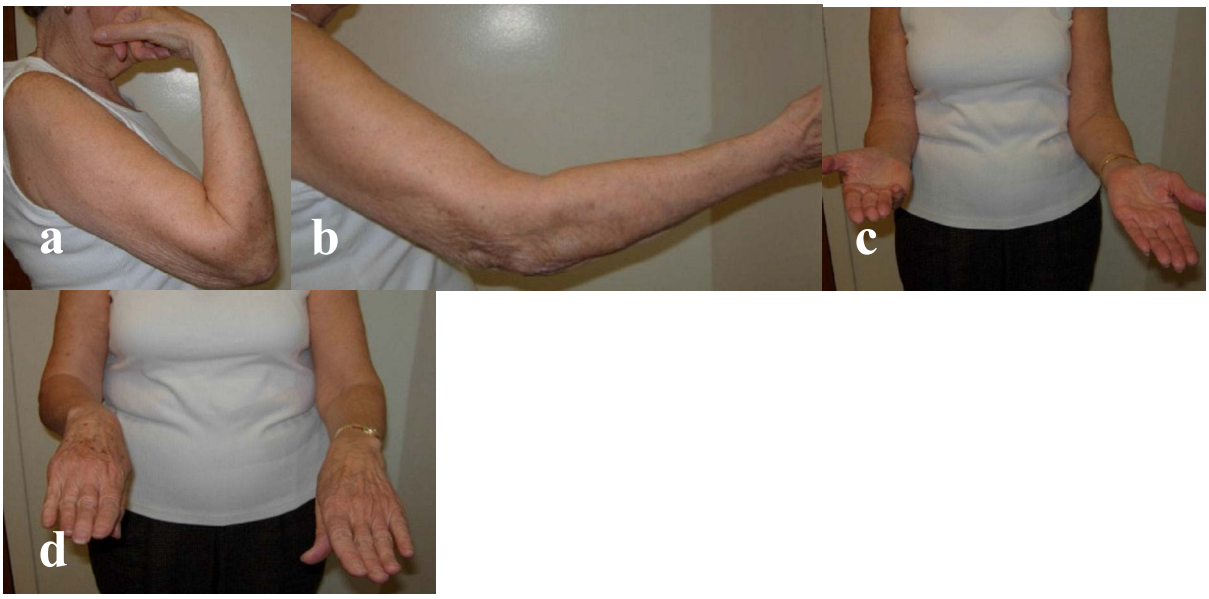

Fig. 13 The patient demonstrated her range-of-motion at six month follow-up. The patient recovered a) 50° of flexion, b) 150° of extension, c) 65° of supination, and d) 80° of pronation.

REFERENCES

1. Horne, J.G. and T.L. Tanzer, *Olecranon fractures: a review of 100 cases.* J Trauma, 1981. **21**(6): p. 469-72.
2. Morrey, B.F., *Current concepts in the treatment of fractures of the radial head, the olecranon, and the coronoid.* Instr Course Lect, 1995. **44**: p. 175-85.
3. Wolfgang, G., et al., *Surgical treatment of displaced olecranon fractures by tension band wiring technique.* Clin Orthop Relat Res, 1987(224): p. 192-204.
4. France, M.P., *Tips of the trade #13. Tension band wiring of olecranon fractures.* Orthop Rev, 1989. **18**(6): p. 713-5.
5. Mullett, J.H., et al., *K-wire position in tension band wiring of the olecranon - a comparison of two techniques.* Injury, 2000. **31**(6): p. 427-31.
6. Macko, D. and R.M. Szabo, *Complications of tension-band wiring of olecranon fractures.* J Bone Joint Surg Am, 1985. **67**(9): p. 1396-401.
7. Wissing, J.C. and C. van der Werken, *[Tension band osteosynthesis of resorbable material].* Unfallchirurg, 1991. **94**(1): p. 45-6.
8. Finsen, V., P.S. Lingaas, and S. Storro, *AO tension-band osteosynthesis of displaced olecranon fractures.* Orthopedics, 2000. **23**(10): p. 1069-72.
9. Lalonde, J.A., Jr., et al., *New tension band material for fixation of transverse olecranon fractures: a biomechanical study.* Orthopedics, 2005. **28**(10): p. 1191-4.
10. Harrell, R.M., et al., *Comparison of the mechanical properties of different tension band materials and suture techniques.* J Orthop Trauma, 2003. **17**(2): p. 119-22.
11. Sarin VK, Mattchen TM, Hack B., *A novel iso-elastic cerclage cable for treatment of fractures.*, in *Proc. 51st Annual Meeting Orthopaedic Research Society*. 2005: Washington, DC.
12. Rothaug, P.G., et al., *A comparison of ultra-high-molecular weight polyethylene cable and stainless steel wire using two fixation techniques for repair of equine midbody sesamoid fractures: an in vitro biomechanical study.* Vet Surg, 2002. **31**(5): p. 445-54.
13. Martin, R., *SecureStrand cable system.* Neurosurgery, 1996. **38**(4): p. 842-3.
14. Molloy, S., et al., *Biomechanical evaluation of intramedullary nail versus tension band fixation for transverse olecranon fractures.* J Orthop Trauma, 2004. **18**(3): p. 170-4.
15. Hutchinson, D.T., et al., *Cyclic loading of olecranon fracture fixation constructs.* J Bone Joint Surg Am, 2003. **85-A**(5): p. 831-7.
16. Prayson, M.J., et al., *Biomechanical comparison of fixation methods in transverse olecranon fractures: a cadaveric study.* J Orthop Trauma, 1997. **11**(8): p. 565-72.